N90-28617

DEVELOPMENT OF AN INTEGRATED BEM FOR HOT FLUID-STRUCTURE INTERACTION

G.F. Dargush
P.K. Banerjee

Department of Civil Engineering
State University of New York at Buffalo
Buffalo, New York 14260

1. INTRODUCTION

One of the most difficult problems in engine structural component durability analysis is the determination of the temperatures and fluxes in the structural components directly in contact with the hot gas flow path. Currently there exists no rational analytical or numerical technique which can effectively deal with this problem. The analysts involved in the hot fluid dynamics who use the finite difference method very rarely interact with those engaged in the thermal analysis of the structural components where the dominant numerical method is the finite element method. Since the temperature distribution in the structural components are strongly influenced by both the fluid flow and the deformation as well as the cooling system in the structure, the only effective way to deal with this problem is to develop an integrated solid mechanics, fluid mechanics and heat transfer analysis for this problem.

In the present work, BEM is chosen as the basic analysis tool principally because the definition of quantities like fluxes, temperatures, displacements, and velocities are very precise on a boundary based discretization scheme. One fundamental difficulty is, of course, that a BEM analysis requires a considerable amount of analytical work which is not present in other numerical methods. During the past year all of this analytical work has been completed and a two-dimensional, general purpose code has been written. This paper summarizes a portion of that work.

2. PREVIOUS WORK

Virtually nothing has appeared in the literature on the analysis of coupled thermoviscous fluid/structure problems via the boundary element method, although some work has been done on the fluid and solid separately. In general, the solid portion of the problem has been addressed to a much greater degree. For example, a boundary-only steady-state thermoelastic formulation was initially presented by Cruse et al (1977) and Rizzo and Shippy (1977). Recently, the present authors

developed and implemented the quasistatic counterpart (Dargush, 1987). Others, notably Sharp and Crouch (1986) and Chaudouet (1987), introduce volume integrals, to represent the equivalent thermal body forces. A similar domain based approach was taken earlier by Banerjee and Butterfield (1981) in the context of the analogous geomechanical problem.

Meanwhile, only a few groups of researchers are actively pursuing the development of boundary elements for the analysis of viscous fluids. The work reported in Piva and Morino (1987) and Piva et al (1987) focuses heavily on the development of fundamental solutions and integral formulations with little emphasis on implementation. On the other hand, Tosaka and Kakuda (1986, 1987), Tosaka and Onishi (1986) have implemented single region boundary element formulations using approximate incompressible fundamental solutions. This latter group has developed sophisticated non-linear solution algorithms, and consequently, are able to demonstrate relatively high Reynolds number solutions.

3. INTEGRAL FORMULATION FOR SOLIDS

3.1 Introduction

In the present section, a surface only time domain boundary element method is described for a thermoelastic body under quasistatic loading. Thus, transient heat conduction is included, but inertial effects are ignored. Formulations have been developed for three-dimensional, two-dimensional and axisymmetric problems (Dargush, 1987), however, only the 2D plane strain case is detailed below.

3.2 Governing Equations

With the solid assumed to be a linear thermoelastic medium, the governing differential equations for transient thermoelasticity can be written:

$$(\lambda+\mu)\,\frac{\partial^2 u_j}{\partial x_i \partial x_j} + \mu\,\frac{\partial^2 u_i}{\partial x_j \partial x_j} - (3\lambda+2\mu)\,\alpha\,\frac{\partial \theta}{\partial x_i} = 0 \qquad (3.1a)$$

$$\rho c_\varepsilon\,\frac{\partial \theta}{\partial t} = k\,\frac{\partial^2 \theta}{\partial x_j \partial x_j} \qquad (3.1b)$$

where

u_i	displacement vector
θ	temperature
t	time

x_i	Lagrangian coordinate
k	thermal conductivity
ρ	mass density
c_ε	specific heat at constant deformation
λ, μ	Lame's constants
α	coefficient of thermal expansion

Standard indicial notation has been employed with summations indicated by repeated indices. For two-dimensional problems considered herein, the Latin indices i and j vary from one to two.

Note that (3.1b) is the energy equation and that (3.1a) represents the momentum balance in terms of displacements and temperature. The theory portrayed by the above set of equations, formally labeled uncoupled quasistatic thermoelasticity, can be derived from thermodynamic principles. (See Boley and Weiner (1960) for details.)

3.3 Integral Representations

Utilizing equation (3.1) for the solid along with a generalized form of the reciprocal theorem, permits one to develop the following boundary integral equation:

$$c_{\beta\alpha}(\xi)u_\beta(\xi,t) = \int_S [\dot{G}_{\beta\alpha} * t_\beta(X,t) - \dot{F}_{\beta\alpha} * u_\beta(X,t)]dS(X) \ . \qquad (3.2)$$

where

α, β	indices varying from 1 to 3
s	surface of solid
u_α, t_α	generalized displacement and traction $u_\alpha = [u_1 \ u_2 \ \theta]^T$ $t_\alpha = [t_1 \ t_2 \ q]^T$
θ, q	temperature, heat flux
$\dot{G}_{\alpha\beta}, \dot{F}_{\alpha\beta}$	generalized displacement and traction kernels (Dargush, 1987)
$c_{\alpha\beta}$	constants determined by the relative smoothness of s at ξ

and, for example, $\dot{G}_{\alpha\beta} * t_\alpha$ denotes a Riemann convolution integral.

3.4 Numerical Implementation

The boundary integral equation (3.2) is an exact statement. No approximations have been introduced other than those used to formulate the boundary value problem. However, in order to apply (3.2) for the solution of practical engineering problems, approximations are required in both time and space.

For the temporal discretization, the time interval from zero to t is divided into N equal increments of duration Δt. Within each time increment, the primary field variables, t_β and u_β, are assumed constant. As a result, these quantities can be brought outside of the time integral. Since the integrand remaining is known in explicit form from the fundamental solutions, the required temporal integration can be performed analytically, and written as

$$G^{N+1-n}_{\beta\alpha}(X-\xi) = \int_{(n-1)\Delta t}^{n\Delta t} G_{\beta\alpha}(X-\xi, t-\tau)\, d\tau \ . \tag{3.3}$$

Combining this, and similar expressions for the $F_{\beta\alpha}$ integral, with (3.2) produces

$$c_{\beta\alpha}(\xi)u^N_\beta(\xi) = \sum_{n=1}^{N} \int_S \left[G^{N+1-n}_{\beta\alpha}(X-\xi)t^n_\beta(X) - F^{N+1-n}_{\beta\alpha}(X-\xi)u^n_\beta(X) \right] dS(X) \ . \tag{3.4}$$

Next, spatial discretization is introduced in order to evaluate the surface integrals appearing in (3.4). In the present implementation, both linear and quadratic boundary elements are available for the description of the geometry, as well as, the primary field variables. Once this is accomplished, the nodal generalized displacements and tractions are brought outside the surface integral and the remaining shape function-kernel products are integrated numerically. Sophisticated, self-adaptive integration algorithms are employed to ensure accuracy and numerical efficiency.

With the discretization of the boundary integral equation, in both time and space, complete, a system of algebraic equations can be developed to permit the approximate solution of the original quasistatic problem. This is accomplished by systematically writing the integral equations at each global boundary node. The ensuing nodal collocation process produces a global set of equations of the form

$$\sum_{n=1}^{N} \left([G^{N+1-n}]\{t^n\} - [F^{N+1-n}]\{u^n\} \right) = \{0\} \ , \tag{3.5}$$

in which $\{t^n\}$ and $\{u^n\}$ are nodal quantities with the superscript referencing the time step index. It should be noted that during this collocation process, the indirect 'rigid body' technique is employed to determine the strongly singular diagonal block of $[F^1]$.

In a well-posed problem, at any time t, the set of global

generalized nodal displacements and tractions will contain exactly 3P unknown components, where P is the total number of functional nodes. Then, as the final stage in the assembly process, equation (3.5) can be rearranged to form

$$[A^1]\{x^N\} = [B^1]\{y^N\} - \sum_{n=1}^{N-1} \left([G^{N+1-n}]\{t^n\} - [F^{N+1-n}]\{u^n\} \right) \qquad (3.6)$$

in which $\{x^N\}$ and $\{y^N\}$ represent the unknown and known nodal components, respectively. In addition, the summation represents the effect of past events. Thus, all quantities on the right-hand side of (3.6) are known at time step N.

It should be emphasized that the entire boundary element method presented, in this section, has involved surface quantities exclusively. A complete solution to the well-posed linear quasistatic problem, with homogeneous properties, can be obtained in terms of the nodal boundary response vectors, without the need for any volume discretization.

4. INTEGRAL FORMULATIONS FOR FLUIDS

4.1 Introduction

Next, attention turns to the hot fluid. During the course of the work, several alternative integral formulations were developed for both incompressible and compressible flow including the effects of thermal coupling. The most promising of these formulations is discussed below.

4.2 Governing Differential Equations for Hot Fluid Flow

Initially, the governing equations for a general compressible, Newtonian fluid are presented. This set will provide the basis for the development of the boundary integral representation. (The derivation of these equations can be found in standard fluid mechanics texts. See Yuan (1967), for example.)

The conservation of mass in the absence of sources and sinks in the medium gives the equation of continuity:

$$\frac{\partial \rho}{\partial t} + \frac{\partial (\rho v_i)}{\partial x_i} = 0 \ . \qquad (4.1)$$

By introducing kinematics and the constitutive law for a Newtonian fluid with constant coefficients of viscosity, the familiar Navier-Stokes equations appear:

$$\rho \left(\frac{\partial v_i}{\partial t} + v_j \frac{\partial v_i}{\partial x_j}\right) = (\lambda+\mu) \frac{\partial^2 v_j}{\partial x_i \partial x_j} + \mu \frac{\partial^2 v_i}{\partial x_j \partial x_j} - \frac{\partial p}{\partial x_i} \,. \tag{4.2}$$

In the above,

v_i	velocity vector
p	pressure
t	time
x_i	Eulerian coordinate
ρ	mass density
λ, μ	viscosity coefficients.

For a non-Newtonian fluid, additional terms appear in (4.2). However, these terms can be conveniently considered as pseudo-body forces, exactly as done in an elastoplastic analysis of a solid.

Next, the balance expressed by the first law of thermodynamics in conjunction with Fourier's law of heat conduction gives the energy equation as

$$\rho c_v \left(\frac{\partial \theta}{\partial t} + v_i \frac{\partial \theta}{\partial x_i}\right) = k \frac{\partial^2 \theta}{\partial x_i \partial x_i} - p \frac{\partial v_i}{\partial x_i} + Y \tag{4.3}$$

where

θ	temperature
k	thermal conductivity
c_v	specific heat at constant volume
Y	viscous dissipation.

Note that in (4.3), the thermal conductivity has been assumed constant. Finally, the equation of state for an ideal fluid is introduced to relate temperature and pressure. That is,

$$p = \rho R \theta \tag{4.4}$$

in which R is a gas constant.

The equations (4.1-4.4) represent a coupled set of five equations with five unknowns, namely v_i, ρ, p and θ.

For the special case of incompressibility, ρ is constant and the continuity condition becomes simply

$$\frac{\partial v_i}{\partial x_i} = 0, \tag{4.5}$$

while the equations of motion reduce to

$$\rho \left(\frac{\partial v_i}{\partial t} + v_j \frac{\partial v_i}{\partial x_j}\right) = \mu \frac{\partial^2 v_i}{\partial x_j \partial x_j} - \frac{\partial p}{\partial x_i} \quad . \tag{4.6}$$

Then, (4.5) and (4.6) form a system of three equations in the unknowns v_i and p. The equations of energy and state are no longer required to determine fluid motion. However, under non-isothermal conditions, the fluid temperatures can be obtained from (4.3) after the velocities are established. The exception, to this two stage approach, is for buoyancy driven flow in which the body forces produced by temperature gradients are dominant. In this latter case, continuity (4.5), momentum (4.6) and energy (4.3) conservation must be satisfied simultaneously.

4.3 Integral Representations

During the early stages of the present work (1986-87), a vorticity formulation was implemented. It was observed that while this formulation has some very convenient features, incorporation of appropriate boundary conditions for a practical problem becomes a difficult task. At the later stages of the current work, it may be possible to incorporate these vorticity integrals within a coupled compressible potential flow - convective heat transfer formulation to provide a very cost effective method for the solution of the present problem. However, before any such approximate method is developed, it is important to examine the full scale implementation of the complete governing equations. With that in mind, recent attention has been directed exclusively toward velocity-pressure-temperature integral formulations.

One of the primary requirements of developing a boundary element formulation is that the fundamental solution of the governing differential equations must exist. These fundamental solutions can be viewed in same sense as the shape functions in the finite element method. For solid mechanics these have been very well explored. Starting with Kelvin's solution (1846), investigators such as Stokes, Poisson, Boussinesq, Mindlin, and Nowacki have provided both static and transient solutions which form the basis of the boundary element formulations in solid mechanics. It is unfortunate that workers in fluid mechanics have not found any use for these fundamental solutions in the infinite space and therefore have not made any attempt to derive such solutions. Since the boundary element formulations could not be developed without these solutions, a substantial amount of effort was devoted in the present work to successively derive more and more complete solutions of the differential equations. As a first approximation the compressibility terms in (4.2) were ignored and the complete fundamental solution for a transient body force and a transient heat source was derived. Details of the derivation can be found in Dargush et al. (1987) or, via an alternate method, in Piva and Morino

(1987). In a subsequent effort these solutions were extended to include the effect of compressibility, although in the latter case, some approximation was necessary.

These fundamental solutions are used in conjunction with a reciprocal identity for fluid dynamics to produce the following integral representation for the velocity:

$$c_{\beta\alpha}(\xi)v_\beta(\xi,\tau) = \int_S \left[\dot{G}_{\beta\alpha} * t_\beta(X,t) - \dot{F}_{\beta\alpha} * v_\beta(X,t) \right] dS(X)$$

$$+ \int_V \left[\dot{G}_{\beta\alpha} * f_\beta(Z,t) \right] dV(Z) \qquad (4.7)$$

where in two-dimensions

$$v_\beta = [v_1 \; v_2 \; \theta]^T$$

$$t_\beta = [t_1 \; t_2 \; q]^T$$

$$f_\beta = [f_1 \; f_2 \; \psi]^T \; .$$

The generalized body forces, f_β, appearing in (4.7), include the convective inertia forces, and in the compressible case, forces due to variable density. The time dependent functions $G_{\beta\alpha}$ and $F_{\beta\alpha}$ can be developed directly from the fundamental solutions.

While the formulation presented above is perfectly valid, two additional modifications have proved quite beneficial. The first involves performing integration by parts on the convective body force. This releases a nonlinear surface integral, but also completely eliminates the need for calculating velocity gradients in incompressible flow. With compressibility, only the scalar dilatation is required. Thus, in both cases, significant computational savings result.

The other modification involves the decomposition of the total velocity into the free stream velocity plus a velocity perturbation. Upon substituting this decomposed form into the governing differential and integral equations, one finds that the volume integration is required only in portions of the flow field in which the total velocity differs from that of the free stream. In a practical sense, this means that, in many problems, volume discretization can be confined to a small region around an obstruction.

4.4 Numerical Implementation

The numerical treatment of the equations in thermoviscous fluid dynamics follows very closely that described in Section 3 for transient

thermal stress analysis. However, now due to the volume integral appearing in (4.7), the interior must be subdivided into cells. The geometry of each cell is defined by nodal points and quadratic shape functions. In two-dimensions, six and eight-noded cells are available. Meanwhile, either a linear or quadratic variation can be employed for the functional representation.

Just as for the thermoelastic case, a set of algebraic equations can be developed by writing the integral equation at each global node. However, now interior, as well as, boundary nodes must be included, and the resulting equations become highly nonlinear due to the convective terms. After the collocation process is complete, the final system of equations can be expressed as

$$A^b x - G^b f = B^b y \tag{4.8a}$$

$$v = A^v x + B^v y + G^v f \tag{4.8b}$$

$$\varepsilon = A^\varepsilon x + B^\varepsilon y + G^\varepsilon f \tag{4.8c}$$

where

x,y are the known and unknown boundary quantities
v are the interior velocity vectors
ε are velocity gradients

An iterative algorithm similar to the initial stress method (Banerjee and Butterfield, 1981) can then be developed as follows:

1. Assume f = 0
2. Increment boundary conditions
3. Calculate the boundary and interior solutions x,v,v and ε
4. Determine f, ψ ,and ρ_v at this time increment
5. Calculate the boundary and interior solutions again
6. If the solution is not significantly different from (3), go to (2); if the solution is different, then go to (4).

Unfortunately, however, convergence is usually achieved with such an algorithm only at low Reynolds number. More generally the interior equations must be brought into the system matrix along with the boundary equations, and a full or modified Newton-Raphson iterative algorithm must be employed to obtain solutions at moderate or high Reynolds number. This type of algorithm has recently been implemented for multi-region flow fields.

5. COUPLING OF SOLID AND FLUID

The coupling of the solid and fluid phases is most readily accommodated via the concept of the generic modeling region. Thus, the

fluid-structure interface is nothing more than a boundary between two GMR's. In the simplest case, temperature, flux, and tractions are matched across the fluid-structure interface, while a temporal approximation is introduced to relate boundary displacements of the solid to the corresponding fluid velocities. However, additional sophistication is possible. For example, thermal resistance can be introduced to model the effects of coatings.

6. NUMERICAL EXAMPLES

6.1 Introduction

All of the formulations discussed above have been implemented as a segment of GP-BEST, a general purpose boundary element code. In this section, a few simple examples are included, primarily, to demonstrate the validity and attractiveness of the boundary element formulations.

6.2 Tube and Fin Heat Exchanger

As a first example, consider the thermal stress analysis of a tube and fin heat exchanger. This type of analysis, under transient conditions, is often required to evaluate the durability of proposed designs. Consider a stainless steel tube with a wall thickness of 0.050in. brazed to a 0.020in. gauge fin of similar material. Figure 6.1 details the geometry. Notice that a fillet radius of 0.015in. is assumed between the tube and fin.

The heat exchanger is cooled continuously by a fluid at $0^{o}F$ flowing inside the tube. It is assumed that this cooling process is of sufficient duration to produce zero temperature, uniformly, throughout the tube and fin. Then, suddenly, at time zero the outer surfaces of the tube and fin are exposed to a $1000^{o}F$ hot gas. The convection coefficients for the inner and outer surfaces are 20 and 10 in.-lb./sec.in^{2o}F, respectively. It should be emphasized that using today's standard technology, these coefficients are determined experimentally or crudely approximated from handbooks.

The following material properties for the metal apply:

$E = 29 \times 10^{6}$ psi, $\nu = 0.30$,
$\alpha = 9.6 \times 10^{-6}/^{o}F$,
$k = 1.65$ in.-lb./sec.in.^{o}F, $\rho c_{g} = 368$ in.-lb./in.^{3o}F .

For the analysis one-half of a single fin is isolated. The two-dimensional boundary element model is depicted in Figure 6.2. The model consists of two Generic Modeling Regions (GMR's) corresponding roughly to the tube plus braze fillet and the fin.

The resulting temperature contours are displayed in Figure 6.3 at

0.25 sec., 0.50 sec., 0.75 sec., and 1.00 sec. As expected, the thin fin, distant from the cold fluid, heats up much more rapidly than the tube. The most severe thermal gradients exist near the braze joint. Von Mises equivalent stresses are plotted in Figure 6.4 for points on the inner tube surface and on the fillet radius.

6.3 Driven Cavity

The two-dimensional driven cavity has become the standard test problem for incompressible computational fluid dynamics codes. In a way, this is unfortunate because of the ambiguities in the specification of the boundary conditions. However, numerous results are available for comparison purposes.

The incompressible fluid of uniform viscosity is confined within a unit square region. The fluid velocities on the left, right and bottom sides are fixed at zero, while a uniform non-zero velocity is specified in the x-direction along the top edge. Thus, in the top corners, the x-velocity is not clearly defined. To alleviate this difficulty in the present analysis, the magnitude of this velocity component is tapered to zero at the corners.

Results are presented for the 144 cell boundary element model shown in Figure 6.5. Notice that a higher level of refinement is used near the edges. Spatial plots of the resulting velocity vectors are displayed in Figures 6.6, 6.7, and 6.8 for Reynolds numbers (Re) of 100, 400 and 1000, respectively. Notice that, in particular, the shift of the vortical center follows that described by Burggraf (1966) in his classic paper. A more quantitative examination of the results can be found in Figure 6.9, where the horizontal velocities on the vertical centerline obtained from the present analysis (i.e., GP-BEST results) are compared to those of Ghia et al. (1982). It is assumed that the latter solutions are quite accurate since the authors employed a 129 by 129 finite difference grid. It is apparent, from the figure, that the present boundary element model has some difficulty in capturing the sharp knee of the curve at Re = 400. This becomes accentuated as the Reynolds number increases, and consequently, a finer mesh is required. It should be noted that the simple iterative algorithm fails to converge much beyond Re = 100. Beyond that range the use of a Newton-Raphson type algorithm is imperative.

6.4 Flow Over a Cylinder

Finally, an example of unconfined flow around an obstacle is considered. In particular, the oft-studied case of a unit diameter circular cylinder is examined. The boundary element mesh is illustrated in Figure 6.10. Notice that three distinct regions are evident. The smallest region, labelled GMR1, represents a thermoelastic thick-walled cylinder. Only the surface of the solid is discretized. The next region, GMR2, models a thermoviscous fluid in the vicinity of the

cylinder. In GMR2 volume cells are required due to convective body forces. However, sufficiently remote from the cylinder, these body forces become negligible and once again a boundary-only region, in this case GMR3, is valid.

Steady-state velocity vector plots are displayed in Figures 6.11 and 6.12 for Re = 20 and 40, respectively. The recirculating zone, behind the cylinder, is clearly visible.

Additionally, the problem was extended to include thermal effects. The temperature of the fluid at inlet was specified as 1000°C, while that at the inner surface of the hollow cylinder was maintained at 0°C. The effective heat transfer coefficient between the fluid and solid can then be obtained from the resulting temperature and flux at the outer surface of the cylinder. The distribution of the nondimensional Nusselt number (Nu) around the circumference is plotted in Figure 6.13. These curves agree, at least, qualitatively with the experimental results of Eckert and Soehngen (1952). Of course, if the purpose of the analysis is to determine the temperature and stress in the solid, then there is really no need to compute the heat transfer coefficients. The desired solid temperatures and stresses come directly out of the analysis.

7. CONCLUSIONS

Boundary element formulations for hot fluid/structure interaction have been developed for the first time and implemented in a general-purpose two-dimensional code. These formulations are attractive primarily because of the ability of the integral method to precisely determine surface behavior at the fluid/structure interface. Additionally, in many instances, only a small portion of the flow field requires domain discretization. Thus, potentially, computational time and modeling effort could be less than with finite difference or finite element techniques.

However, much work remains. For example, the compressible formulation must be tested and a variety of techniques, analogous to upwinding, must be investigated in order to push solutions to the Reynolds number range of interest for SSME and beyond.

REFERENCES

Banerjee, P.K. and Butterfield, R. (1981), 'Boundary Element Methods in Engineering Science,' McGraw-Hill, London.

Boley, B.A. and Weiner, J.H. (1960), 'Theory of Thermal Stresses,' John Wiley and Sons, New York.

Burggraf, O. (1966), 'Analytical and Numerical Studies of the Structure of Steady Separated Flows,' J. Fluid Mech., V24, Part 1, pp. 113-151.

Chaudouet, A. (1987), 'Three-dimensional Transient Thermo-elastic Analysis by the BIE Method,' Int. J. Num. Meth. Engrg., V24, pp. 25-45.

Cruse, T.A., Snow, D.W. and Wilson, R.B. (1977), 'Numerical Solutions in Axisymmetric Elasticity,' Comp. and Struct., V7, pp. 445-451.

Dargush, G.F. (1987), BEM for the Analogous Problems of Thermoelasticity and Soil Consolidation, Ph.D. Dissertation, State University of New York at Buffalo.

Dargush, G., Banerjee, P.K. and Dunn, M.G (1987), Development of an Integrated BEM Approach for Hot Fluid Structure Interaction,NASA Annual Report.

Eckert, E.R.G. and Soehngen, E. (1952), 'Distribution of Heat-Transfer Coefficients Around Circular Cylinders in Crossflow at Reynolds Numbers From 20 to 500,' Transactions of the ASME, V74, pp. 343-347.

Ghia, U., Ghia, K.N. and Shin, C.T. (1982), 'High-Re Solutions for Incompressible Flow Using the Navier-Stokes Equations and a Multigrid Method,' J. Comp. Physics, V48, pp. 387-411.

Piva, R., Graziani, G. and Morino, L. (1987) 'Boundary Integral Equation Method for Unsteady Viscous and Inviscid Flows,' IUTAM Symposium on Advanced Boundary Element Method, San Antonio, Texas.

Piva, R. and Morino, L. (1987), 'Vector Green's Function Method for Unsteady Navier-Stokes Equations,' Meccanica, Vol. 22, pp. 76-85.

Rizzo, F.J. and Shippy, D.J. (1977), 'An Advanced Boundary Integral Equation Method for Three-dimensional Thermoelasticity,' Int. J. Num. Meth. Eng., V11, pp. 1753-1768.

Sharp, S. and Crouch, S.L. (1986), 'Boundary Integral Methods for Thermoelasticity Problems,' J. Appl. Mech., V53, pp. 298-302.

Tosaka, N., and Kakuda, K. (1986), 'Numerical Solutions of Steady Incompressible Viscous Flow Problems by Integral Equation Method,' pp. 211-222 in R.P. Shaw et.al., Eds., Proc. 4th Intl. Symp. Innov. Num. Methods Engrg., Springer, Berlin.

Tosaka, N. and Kakuda, K. (1987), 'Numerical Simulations of Laminar and Turbulent Flows by Using an Integral Equation,' Boundary Elements IX, eds. Brebbia, Wendland and Kuhn, pp. 489-502.

Tosaka, N. and Onishi, K. (1986), 'Boundary Integral Equation Formulations for Unsteady Incompressible Viscous Fluid Flow by Time-differencing,' Engineering Analysis, V3, No. 2, pp. 101-104.

Yuan, S.W. (1967), 'Foundations of Fluid Mechanics,' Prentice-Hall, New Jersey.

FIGURE 6.1

TUBE AND FIN HEAT EXCHANGER

Problem Definition

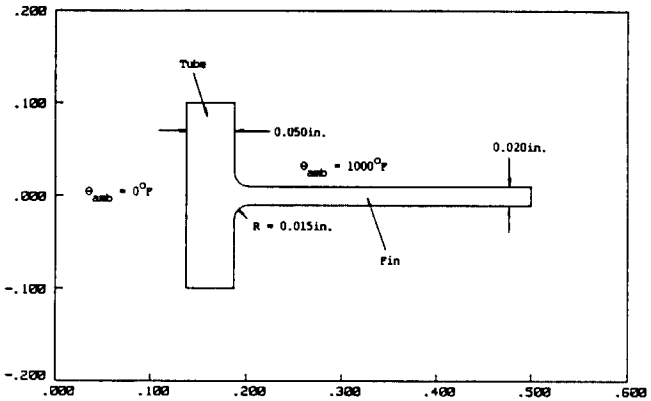

FIGURE 6.2

TUBE AND FIN HEAT EXCHANGER

Boundary Element Model

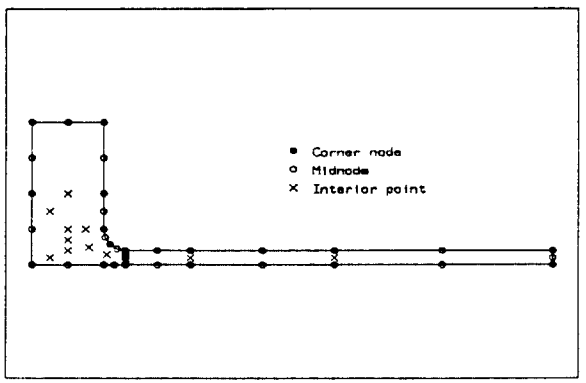

FIGURE 6.3 - TUBE AND FIN HEAT EXCHANGER - TEMPERATURE CONTOURS

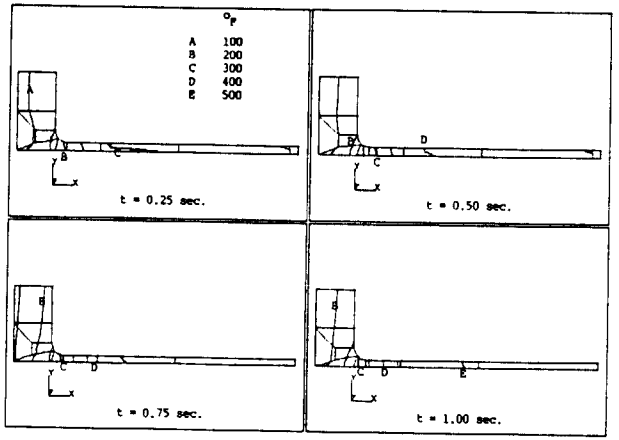

FIGURE 6.4

TUBE AND FIN HEAT EXCHANGER

Stress Results

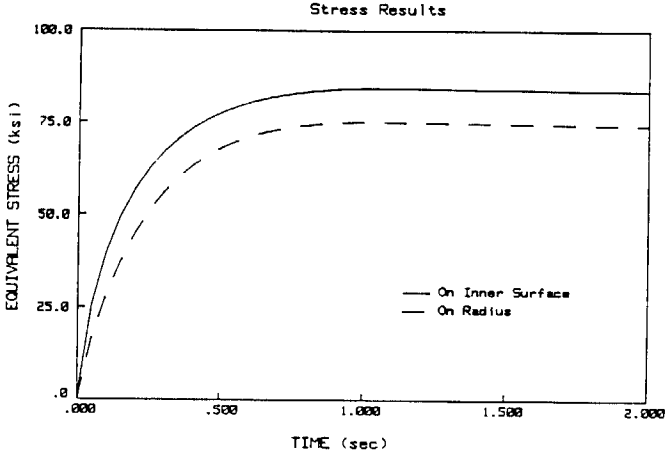

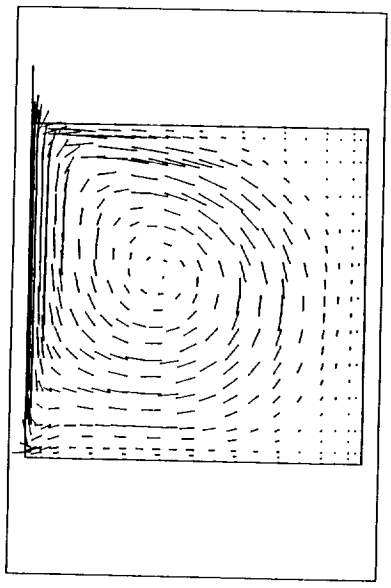

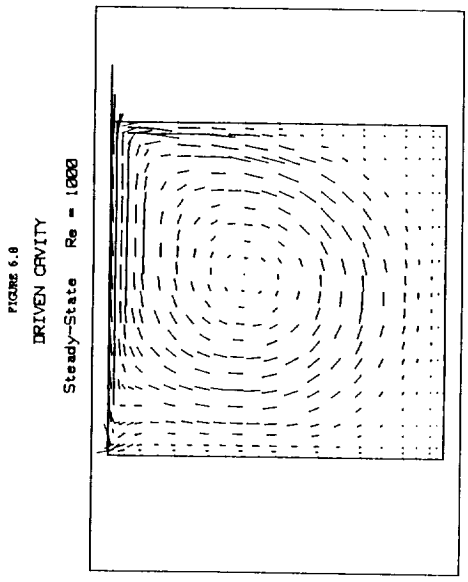

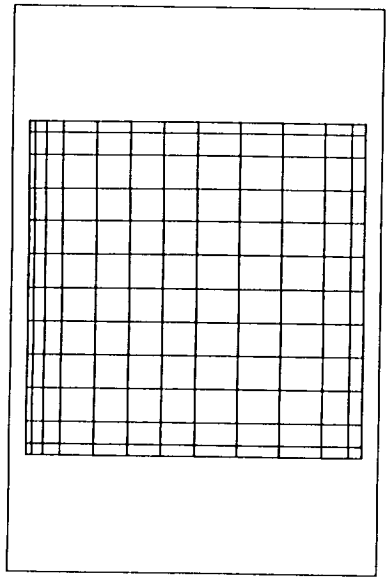

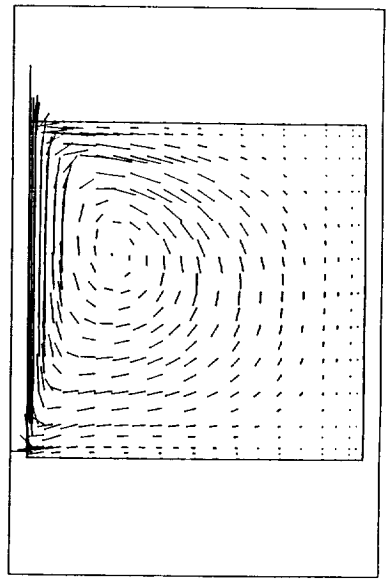

FIGURE 6.9

DRIVEN CAVITY

VELOCITY PROFILE

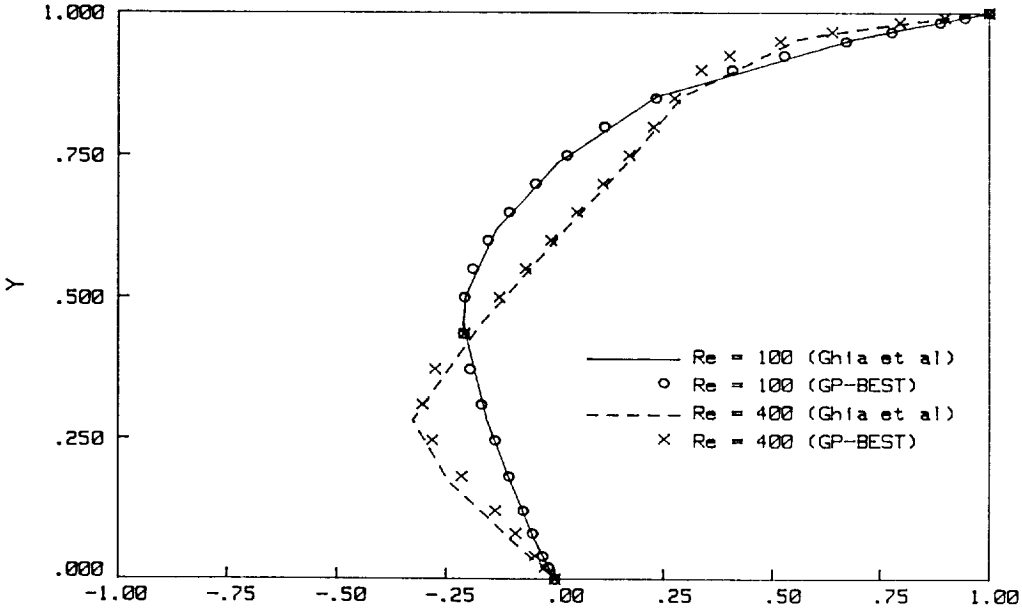

FIGURE 6.10

FLOW AROUND A CYLINDER

Boundary Element Model

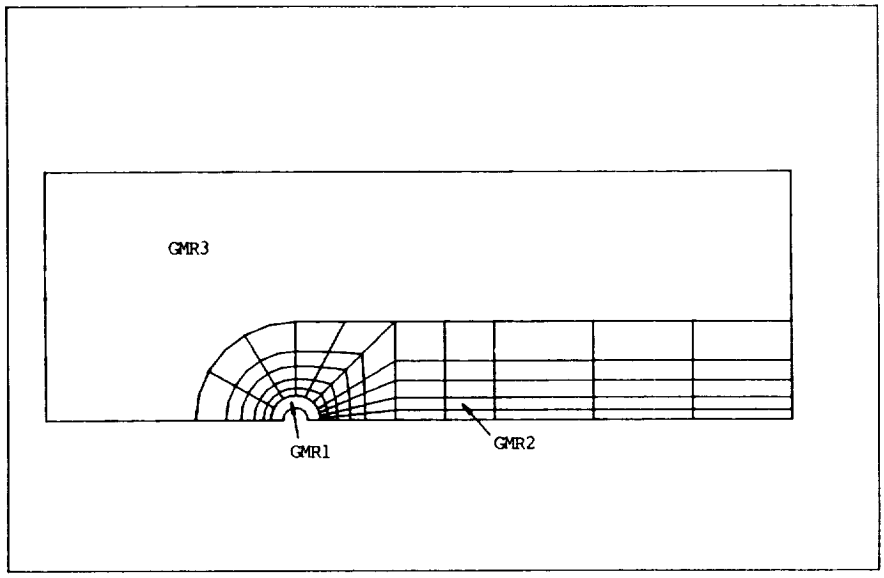

FIGURE 6.11a

FLOW AROUND A CYLINDER

Re = 20

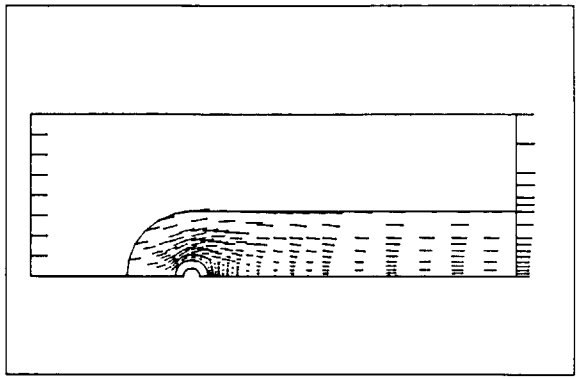

FIGURE 6.11b

FLOW AROUND A CYLINDER

Re = 20

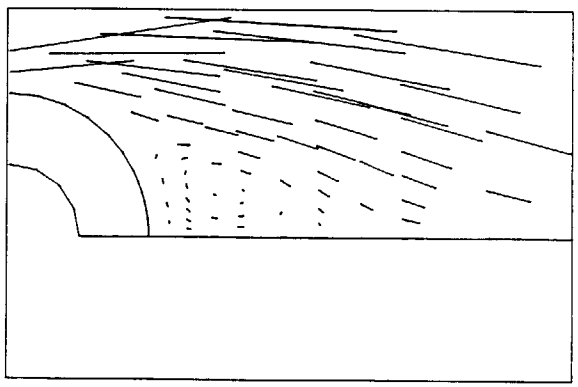

FIGURE 6.12a

FLOW AROUND A CYLINDER

Re = 40

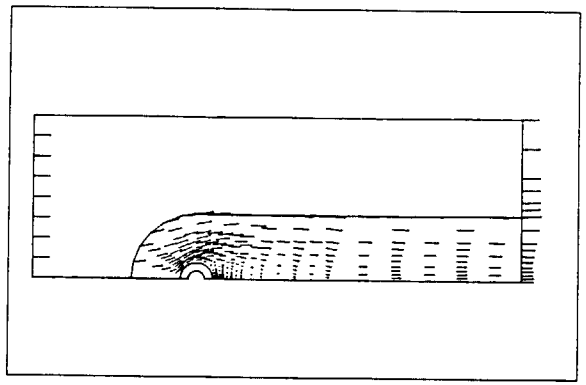

FIGURE 6.12b

FLOW AROUND A CYLINDER

Re = 40

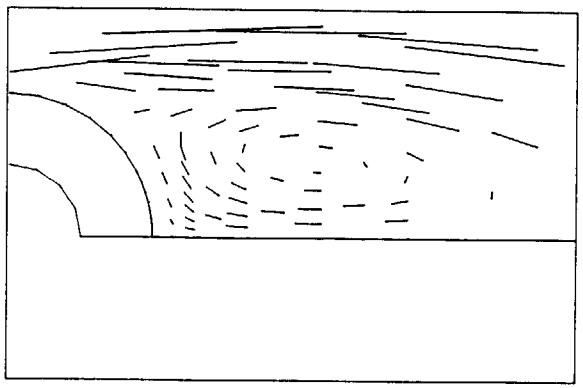

FIGURE 6.13

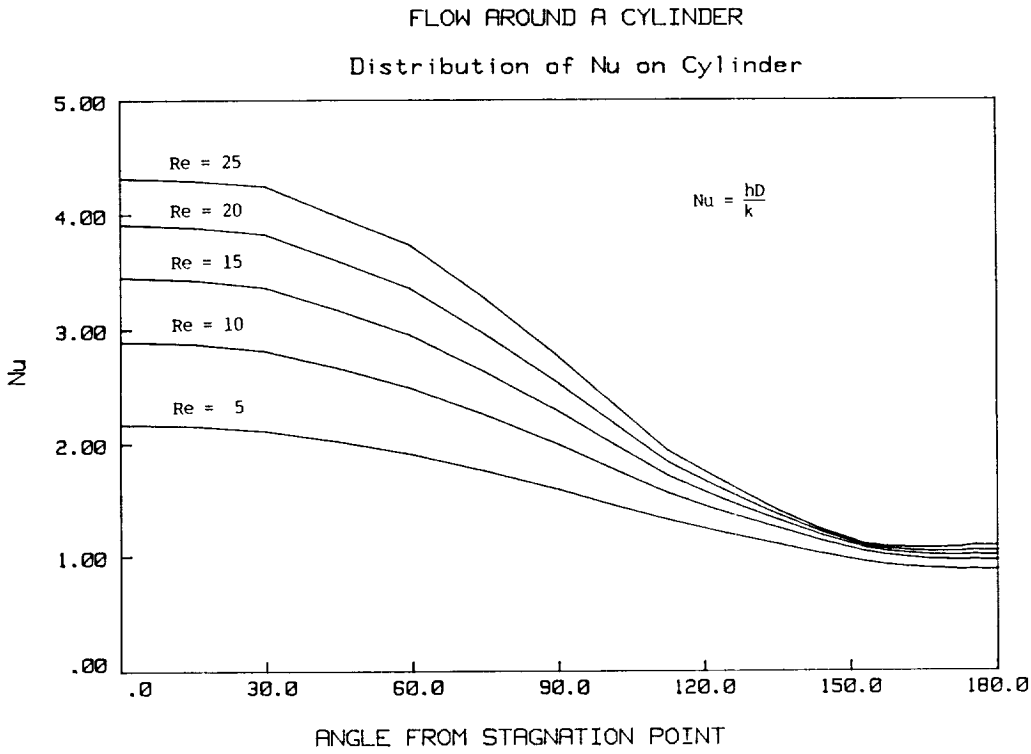
FLOW AROUND A CYLINDER
Distribution of Nu on Cylinder
5.00
4.00
3.00
2.00
1.00
.00
Nu
Re = 25
Re = 20
Re = 15
Re = 10
Re = 5
Nu = hD/k
.0
30.0
60.0
90.0
120.0
150.0
180.0
ANGLE FROM STAGNATION POINT